Int J Adv Manuf Technol (2015) 78:1437–1443
DOI 10.1007/s00170-014-6748-9

ORIGINAL ARTICLE

Effect of friction stir processing with B_4C particles on the microstructure and mechanical properties of 6061 aluminum alloy

Yong Zhao · Xiaolu Huang · Qiming Li · Jian Huang · Keng Yan

Received: 2 June 2014 / Accepted: 19 December 2014 / Published online: 10 January 2015

Abstract In this paper, friction stir processing (FSP) with B_4C particles (B_4C_p) is used to improve the surface modification of 6061 aluminum alloy. Optical microscopy, scanning election microscopy, and energy-dispersive X-ray analysis have been performed to investigate the microstructure and the distribution of B_4C_p. Wear resistance and microhardness were evaluated in detail. It is observed that the increasing number of FSP passes causes a more uniform distribution of B_4C_p. The homogeneous distribution of B_4C_p was observed in the weld zone, which significantly improved the wear resistance and microhardness of the surface composite layer as compared to those of the as-received Al alloy.

Keywords Friction stir processing · B_4C particles · 6061 aluminum alloy · Microstructure · Microhardness

1 Introduction

Aluminum alloys are used widely in aerospace and automotive industries because of their low density and high strength to weight ratio. However, the mechanical properties of aluminum alloys, such as hardness and resistance to wear, are not sufficient to enhance their applications [1, 2]. In recent years, many surface modification technologies were used for the fabrication of metal matrix surface composite layers, mainly including laser cladding technology, ion implantation technology, plasma spraying technology, micro-arc oxidation technology [3–6], and so on. However, the laser cladding technology for forming surface composites is based on liquid phase processing at high temperatures. In this case, it is hard to avoid the interfacial reaction between reinforcement and metal matrix and the formation of some detrimental phases. When using micro-arc oxidation or spraying techniques, there is an obvious stratification between the surface layer and the parent metal and the interfacial bonding strength is limited. Using the ion implantation method, the thickness of the surface composite layer is only a few hundred nanometers.

Friction stir processing (FSP) based on friction stir welding is a solid-state technique used for material processing in order to modify microstructures and mechanical properties. Also, it is possible to produce a surface composite layer by this process [7]. The processing of a surface composite by FSP is carried out at temperatures below the melting point of the substrate, so the problems mentioned above can be avoided. As the rotating tool traverses on the surface of the matrix, the metal is essentially extruded around the tool and can be plastically deformed easily. Then, a surface composite layer with a microstructure of densification, homogenization, and grain refinement is got, the strengthening particles are well distributed in the matrix, and good bonding with the matrix is generated. Typically, the thickness of the composite layer can reach a few millimeters. Hsu et al. [8] produced an Al–Al_3Ti nanocomposite layer by FSP and improved the Young modulus and the tensile strength of aluminum. They showed that the Young modulus of the Al–Al_3Ti composite increases significantly with increasing volume fraction of Al_3Ti in the matrix. Asadi et al. [9] used FSP to fabricate a SiC/AZ91 composite layer and investigated the effect of

Y. Zhao · Q. Li · J. Huang (✉)
Shanghai Key Laboratory of Materials Laser Processing and Modification, School of Materials Science and Engineering, Shanghai Jiao Tong University, Shanghai 200240, China
e-mail: jhuang@sjtu.edu.cn

Y. Zhao · X. Huang · Q. Li · K. Yan
Provincial Key Lab of Advanced Welding Technology, School of Materials Science and Engineering, Jiangsu University of Science and Technology, Zhenjiang 212003, Jiangsu, China

process parameters such as rotational and traverse speeds, tool penetration depth, and tilt angle on the formation of defects such as cracks and tunneling cavity. Asadi et al. [10] investigated the role of cooling and tool rotational direction in the microstructure and mechanical properties of friction stir-processed AZ91. Morisada et al. [2, 11] and Chang et al. [12, 13] similarly investigated the microstructure and the mechanical properties of friction stir-processed AZ31 magnesium.

The objective of this paper is to investigate the possibility of incorporation of B_4C particles (B_4C_p) into the surface layer of 6061 Al alloy to form metal matrix composites by means of the FSP technique. The microstructure and microhardness on the welding zone are evaluated. Also, the wear resistance of the surface composite layer is also examined.

2 Experimental procedures

The thickness of the base metal was 12 mm. To insert B_4C powder, a groove with 2-mm depth and 1-mm width on the 6061 plate was machined out of workpieces, in which the desired amount of B_4C powder was filled in before the FSP was carried out. The average size of the B_4C_p was about 5~7 μm. The chemical composition of 6061 Al alloy is shown in Table 1.

The friction stir process was conducted with a W9Mo3Cr4V steel tool consisting of a concave 14-mm-diameter shoulder and a 5-mm-diameter pin with the length of 2.7 mm. During the FSP, a constant tile angle of 2.5° was maintained. The welding speed was 100 mm/min and the rotation speed of the tool was 1200 rpm. Samples were fabricated by one FSP pass, two FSP passes, three FSP passes, and four FSP passes, respectively.

The joints were cross-sectioned perpendicular to the welding direction for microstructure analyses. The cross sections of the metallographic specimens were etched with Keller's reagent. Scanning electron microscopy (SEM) and optical microscopy (OM) were conducted to investigate the microstructures of the weld zone. The Vickers microhardness measurements were performed across the joints using a 9.81-N load for 30 s to determine the hardness profiles and the hardness variations near the weld zone.

The wear tests were conducted with a pin-on-disk tribometer as shown in Fig. 1. Two pins were made of the materials under study (6061 Al alloy and its surface B_4C composite layer produced by FSP) with a rectangular section of 7 mm×7 mm. The counterpart disks were made of W9Mo3Cr4V steel with the hardness of about 60 HRC and surface roughness of R_a=0.2 μm. Before the wear test, each pin specimen was ground down to 1000-grit abrasive paper. The wear tests were conducted under dry sliding conditions for 3600 s with a constant load (100 N) and sliding velocity (120 r/min). All wear test specimens were cleaned in acetone and weighed to an accuracy of ±1 mg prior to testing. The coefficient of friction between the pin specimen and the disk was determined by measuring the frictional force with a stress sensor.

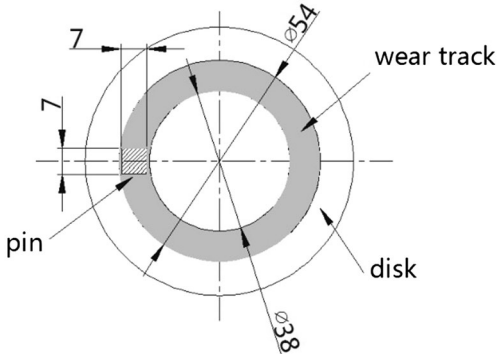

Fig. 1 Scheme of the testing configuration of the pin-on-disk tribometer

Table 1 Chemical composition of 6061 Al alloy (wt.%)

Mg	Si	Cu	Fe	Mn	Cr	Zn	Ti	Al
0.8~1.2	0.4~0.8	0.15~0.4	0.7	0.15	0.04~0.35	0.25	0.15	Bal.

3 Results and discussion

3.1 Microstructures

Figure 2 shows the macroscopic overview of the cross section of the friction stir-welded AA6061/B_4C_p composite fabricated by the FPS with different passes. As shown in Fig. 2a, b, B_4C particles are located at the bottom of the weld zone with one and two FSP passes. No B_4C particles are observed in the upper region of the weld zone. This phenomenon may be caused by insufficient mixing. The arrow-pointed dark regions in Fig. 2a, b are agglomerated B_4C particles. Agglomerated B_4C particles could be observed in the surface composite layer produced by one FSP pass and two FSP passes. With three FSP passes, the agglomeration of B_4C particles disappeared and a small amount of B_4C particles appears in the upper weld zone as shown in Fig. 2c. Figure 2d shows the surface composite layer fabricated by four FSP passes. Different from the surface composite layer fabricated by one FSP pass, the region at the bottom of the weld zone extended with uniformly distributed B_4C particles, and the upper region of the weld zone with well-distributed B_4C particles (a thickness of 1 mm) was obtained.

FSP is a solid-state condition in which the rotating tool imparts severe plastic deformation to the workpiece [14]. During the FSP, the particles are wrapped in and flow together

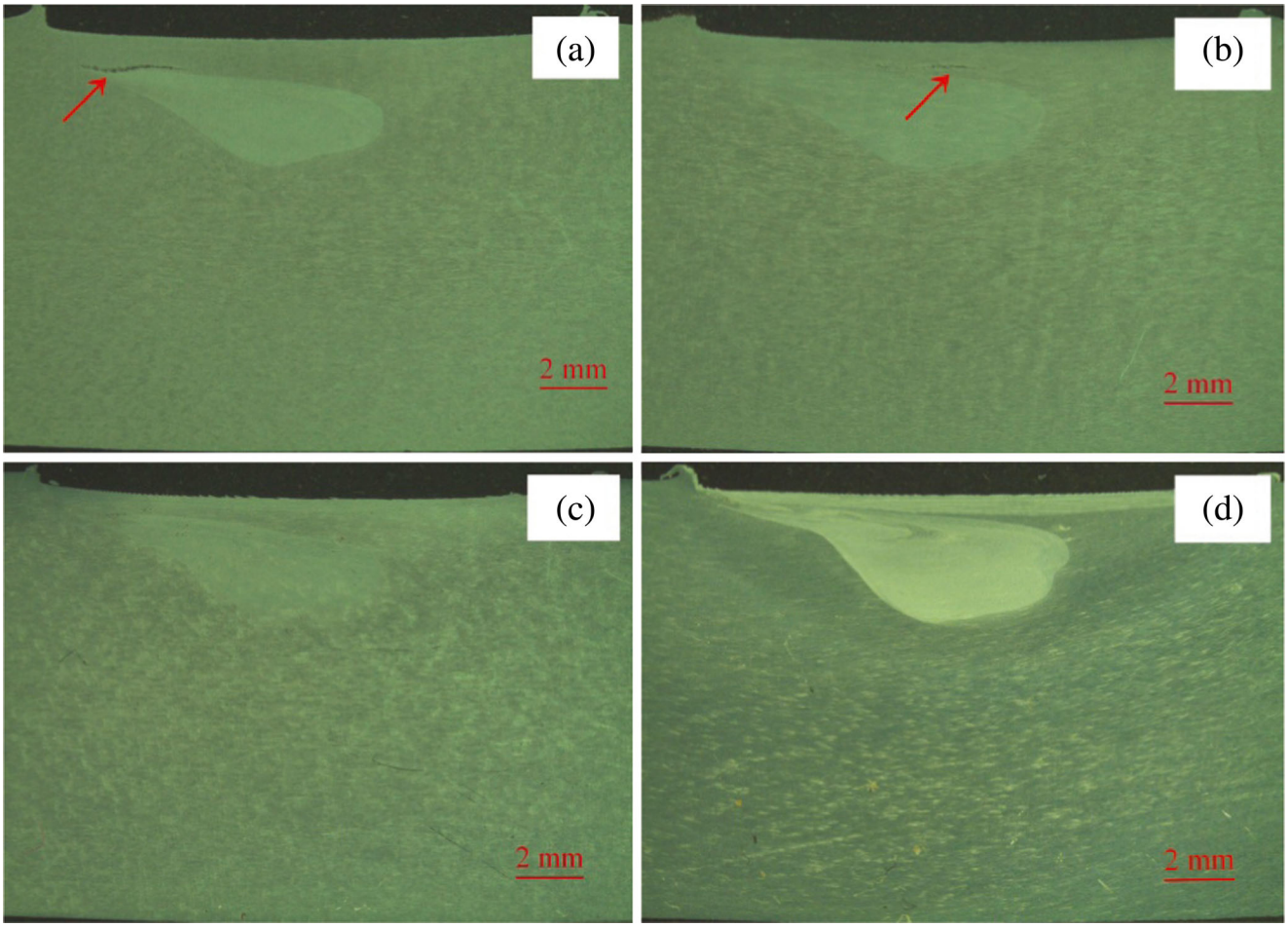

Fig. 2 Macroscopic overview of the cross section of the friction stir-welded AA6061/B_4C_p composite produced by **a** one, **b** two, **c** three, and **d** four FSP passes

with plastic metal. As the significant difference in physical properties between particles and base metal, it is hard for particles to travel with the trail left by the plastic metal [15]. That is why the B_4C particles cannot be easily dispersed and the agglomeration of B_4C particles occurs. So it was essential to fabricate the surface composite layer by four FSP passes.

Figure 3 shows the microstructure of the surface composite layer fabricated by one and two FSP passes. The massive particles in Fig. 3a, b are formed by the agglomerated B_4C particles. However, the agglomeration phenomenon in Fig. 3b is not so serious as that in Fig. 3a. Also, some fine B_4C particles were well incorporated into the as-received Al. With three and four FSP passes, the agglomeration of B_4C particles disappeared as shown in Fig. 3c, d. It is likely that the dispersion of the B_4C particles in the 6061 Al matrix is related to the number of FSP passes. Table 2 illustrates the energy-dispersive X-ray (EDS) analysis result taken from the rectangular region in Fig. 3. The result shows that there are many elements, such as B, C, O, Mg, Al, Si, and S, in the rectangular region. The elements O and S may come from impurities that have not been cleaned up.

The B_4C reinforcement particles were successfully incorporated into the AA6061 matrix by four FSP passes. The microstructure of the AA6061/B_4C_p surface composite layer was characterized by homogeneously distributed B_4C particles as shown in Figs. 4 and 5. The interface between the AA6061/B_4C_p composite layer and the AA6061 matrix was sound without exfoliations. The thermo-mechanically affected zone (TMAZ) was characterized by the B_4C particle-free regions of the surface composite layer. The B_4C particle alignment was also observed in the TMAZ region in Fig. 4, as the TMAZ had been plastically deformed. The distribution of the B_4C_p in the nugget region is more homogeneous, suggesting that the arrangement of the particles had taken place during friction stir welding due to the high deformation and stirring.

Figure 5 shows EDS analysis points defined on the SEM microstructure of the AA6061/B_4C_p composite produced by four FSP passes in the weld nugget. Table 3 illustrates the EDS analysis results taken from point a, which represented the B_4C particle, and point b, which represented the AA6061 matrix alloy. EDX analysis and SEM examination suggest

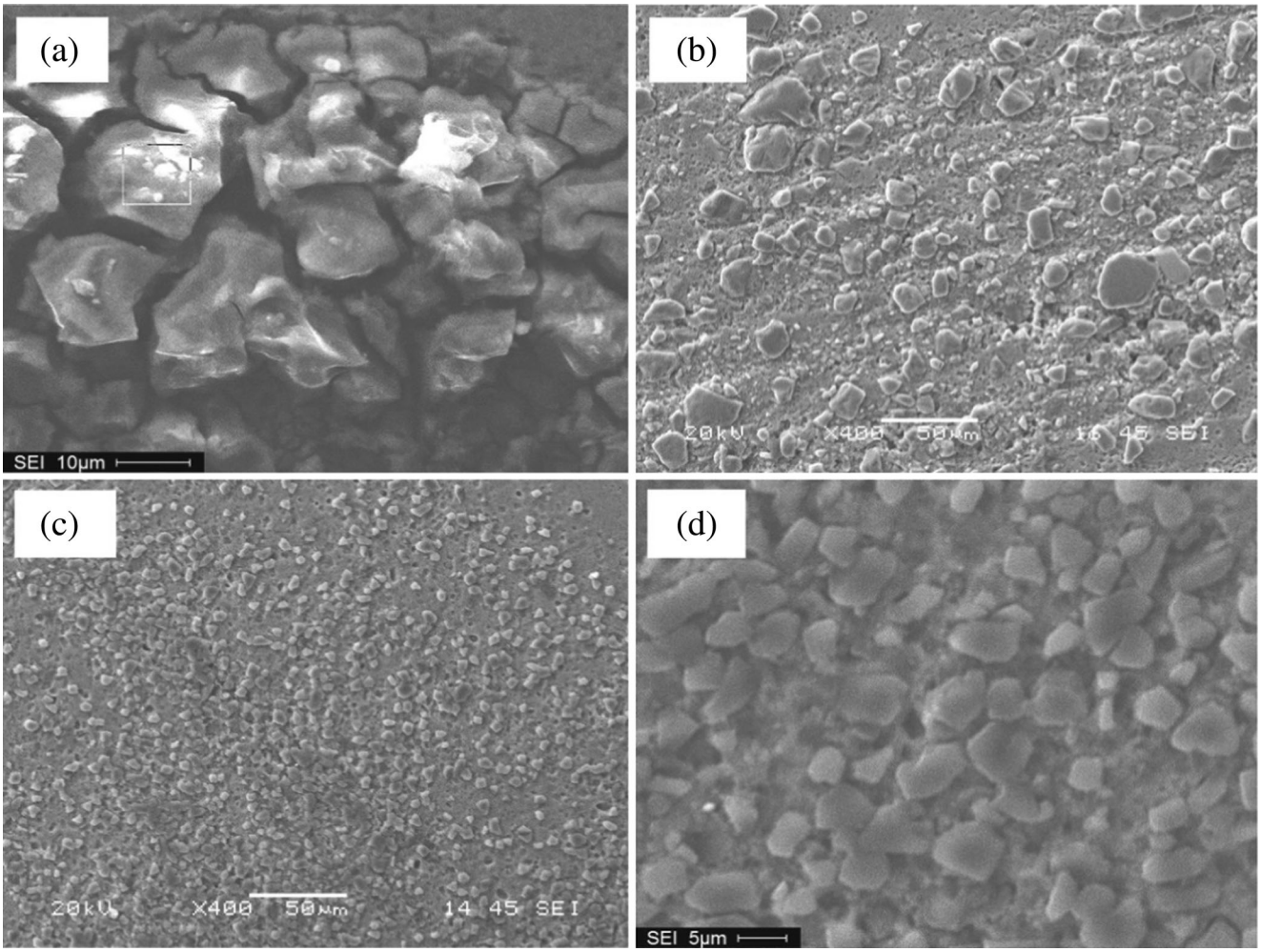

Fig. 3 SEM microstructures and EDS phase analysis of the surface composite layer fabricated by **a** one, **b** two, **c** three, and **d** four FSP passes

that the B_4C particle is 8 μm in size. The test points are composed of Al, O, S, Si, Mg, etc. In particular, the elements Al, Mg, and Si come from the AA6061 matrix alloy. While the elements O and S may have come from outside impurities. It is considered that some B_4C particles were smashed by the rotating tool during the FSP. This is the reason why the point is mainly composed of elements B and C.

3.2 Microhardness distributions

Figure 6 shows the hardness measurement line. Figure 7 shows the microhardness distribution of the parent 6061 Al alloy produced by four FSP passes across the weld zone measured along with the centerline. The as-received AA6061 exhibits a hardness of 51–57 HV. However, the weld zone reaches a higher average hardness of 98 HV with only a small fluctuation in the hardness, indicating that B_4C powders were uniformly dispersed in the weld zone.

Taking the microstructure of the weld zone into account, the reasons for the increasing hardness of the AA6061/B_4C_p

Table 2 Results of EDS analysis of Fig. 3 (wt.%)

B	C	O	Mg	Al	Si	S
20.6	7.75	42.28	0.55	22.45	0.06	6.31

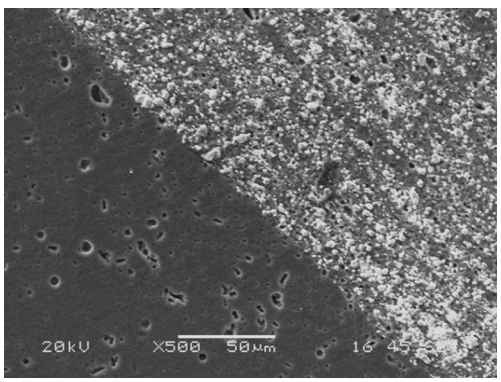

Fig. 4 Microstructure of the AA6061/B_4C_p composite: thermo-mechanically affected zone

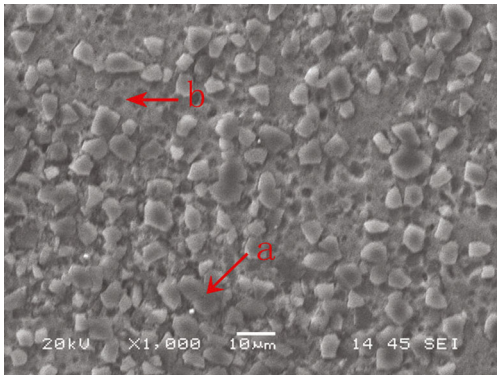

Fig. 5 SEM microstructure of the AA6013/B_4C_p composite in the weld nugget

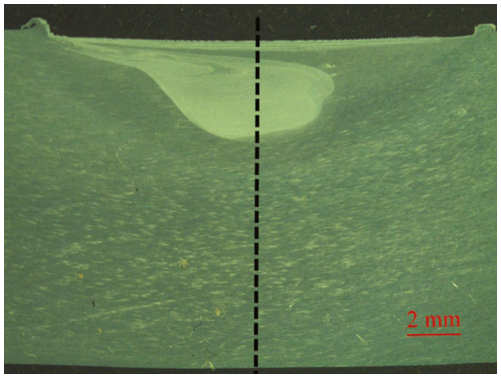

Fig. 6 Hardness measurement line

surface composite layers fabricated by FSP are (1) grain strengthening: the refinement of the grains in the weld zone (the SZ and the TMAZ) and (2) the Orowan strengthening: the fine dispersion of B_4C particles in the weld zone [16].

For the 6061 Al alloy fabricated by four FSP passes, it is observed that there is a reduction of hardness in the heat-affected zone (HAZ) in contrast to that of the as-received 6061 Al alloy. The hardness of the as-received 6061 Al alloy has an average of 53 HV. However, the hardness of HAZ shows a variable value from 39 to 44 HV with an average of 42 HV. It is considered that the softening of the HAZ is a result of grain growth and coarsening of the second phase caused by thermal conditions.

3.3 Wear

Figure 8 shows the weight loss of two specimens with sliding distance using W9Mo3Cr4V steel as the disk material and the specimen as the pin. From Fig. 8, it is observed that the wear weight loss of the two specimens increased with sliding distance. Further analysis of the graph in Fig. 8 shows that the wear properties of the AA6061/B_4C_p surface composite layer are far better than those of the as-received AA6061 substrate.

In order to understand the mechanism of the two specimens, the friction coefficient of the AA6061/B_4C_p surface composite layer fabricated by four FSP passes and the as-received AA6061 substrate and the scanning electron micrograph of the worn surfaces were further studied.

Figure 9 shows the friction coefficient with sliding distance of the AA6061/B_4C_p surface composite layer and the as-received AA6061 substrate. It is obvious that the friction

Table 3 Results of EDS analysis of Fig. 5 (wt.%)

Location	B	C	O	Mg	Al	Si	S
a	80.71	8.01	1.15	0.10	9.69	0.06	0.28
b	12.37	5.56	0.73	1.44	79.40	0.30	0.21

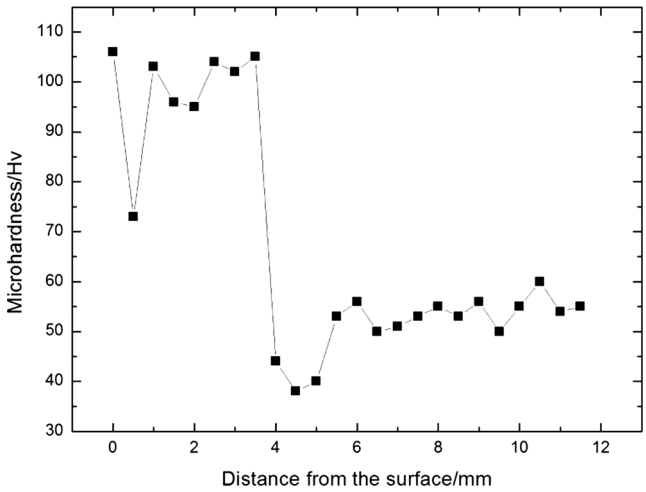

Fig. 7 Hardness distribution near the weld zone

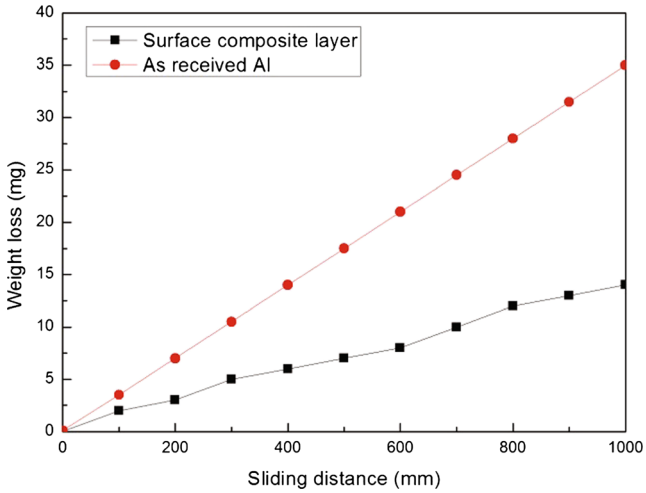

Fig. 8 Weight loss of two specimens with sliding distance

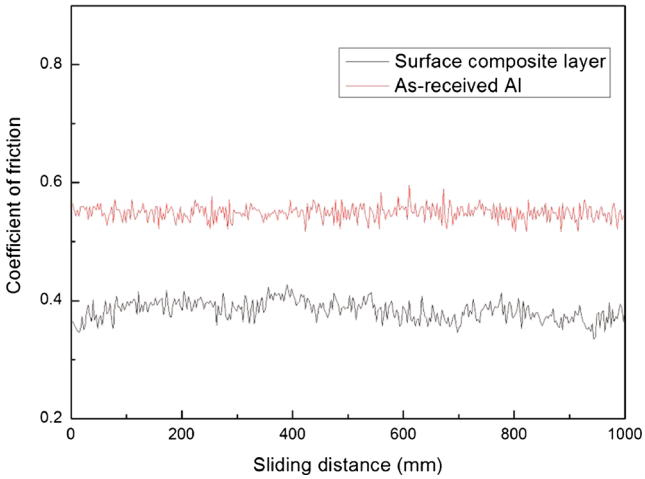

Fig. 9 Variation of friction coefficient with sliding distance

coefficient of the AA6061/B_4C_p surface composite layer is considerably low and remains stable with sliding distance. The average friction coefficient of the surface composite layer is 0.35, which is significantly lower than that of the as-received Al (with an average of 0.55).

Figure 10 shows the scanning electron micrographs of the worn tracks of the as-received AA6061 substrate and the AA6061/B_4C_p surface composite layer against W9Mo3Cr4V steel disk. Fig. 10a shows evidence of the presence of deep scratches in the worn surface. Hence, the mechanism of wear is predominantly abrasive in nature due to the harder (steel disk) surface scratching over the softer (pin) surface. It is also visible that the depth of scratches decreased in the AA6061/B_4C_p surface composite layer as compared to the AA6061 substrate.

The possible reasons for the excellent wear property may be as follows:

(1) Increasing hardness of the AA6061/B_4C_p surface composite layer compared to the as-received AA6061 substrate. The fine dispersion of B_4C particles and the refinement of the grains in the weld zone make an important contribution to the excellent wear property. It is recognized that the wear resistance of materials increases with their hardness [17].

(2) As the hard B_4C particles act as the load-bearing component, the direct load contact between the AA6061/B_4C_p composite surface and the W9Mo3Cr4V steel disk in comparison with the as-received AA6061 metal is greatly reduced, and it helps to reduce the extent of wear [18].

4 Conclusions

The B_4C particle-dispersed AA6061 was successfully fabricated by four FSP passes. The microstructure, microhardness, and wear properties of the AA6061/B4C_p surface composite layer have been studied in the present work. The following conclusions have been drawn:

(1) With increasing number of FSP passes, the dispersion of B_4C particles becomes more uniform. By way of four FSP passes, the expected AA6061/B_4C_p surface composite layer is successfully fabricated with homogeneously distributed B_4C particles in the weld zone. Good bonding with the matrix is generated.

(2) The weld zone shows a higher average hardness of 98 HV and only a small fluctuation in the hardness. It is due to the grain refinement and the uniform distribution of reinforcement particles.

(3) The friction coefficient of the AA6061/B_4C_p surface composite layer produced by four FSP passes is very low compared to that of the base metal. The wear property of the surface composite layer is greatly improved. The improvement of the surface composite layer in wear property is the result of improved hardness and the dispersion of hard B_4C particles in the surface composite layer.

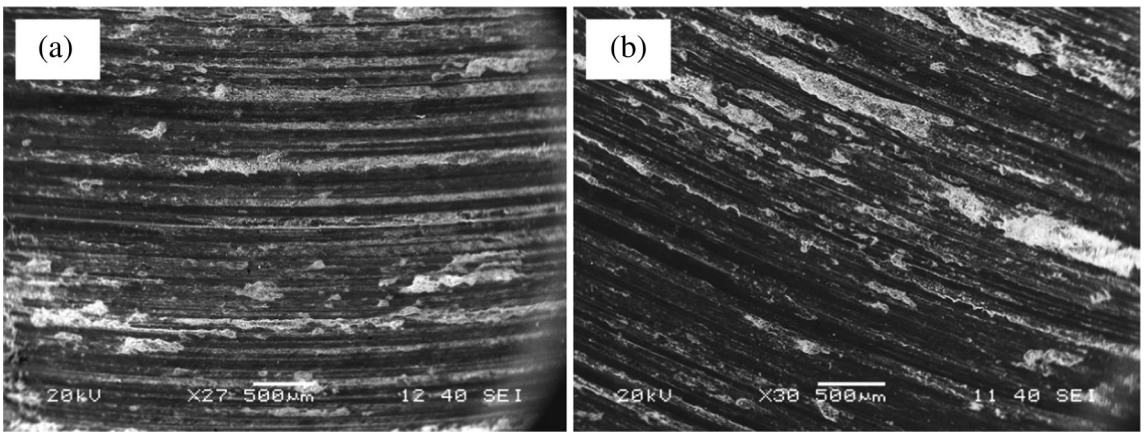

Fig. 10 SEM of the worn surface. **a** As-received Al. **b** Surface composite layer produced by four FSP passes

References

1. Asadi P, Faraji G, Besharati MK (2010) Producing of AZ91/SiC composite by friction stir processing (FSP). Int J Adv Manuf Technol 5:241–260
2. Morisada Y, Fujii H, Nagaoka T, Fukusumi M (2006) Effect of friction stir processing with SiC particles on microstructure and hardness of AZ31. Mater Sci Eng A 433:50–54
3. Santos TG, Miranda RM, Pedro V, Pamies Teixeira J (2011) Modification of electrical conductivity by friction stir processing of aluminum alloys. Int J Adv Manuf Technol 57:511–519
4. Ma ZY (2008) Friction stir processing technology: a review. Metall Mater Trans A 36A:642–658
5. Hulbert D, Fuller C, Mahoney M, London B (2007) The mechanical and thick section bending behavior of friction stir processed aluminum plate. Scripta Mater 57:269–272
6. Charit I, Mishra RS (2005) Low temperature superplasticity in a friction-stir-processed ultrafine grained Al–Zn–Mg–Sc alloy. Acta Mater 53:4211–4223
7. Barmouza M, Asadia P, Besharati Givia MK, Taherishargh M (2011) Investigation of mechanical properties of Cu/SiC composite fabricated by FSP: effect of SiC particles' size and volume fraction. Mater Sci Eng A 528:1740–1749
8. Hsu CJ, Chang CY, Kao PW, Ho NJ, Chang CP (2006) Al-Al3Ti nanocomposites produced in situ by friction stir processing. Acta Mater 54:5241–5249
9. Asadi P, Faraji G, Besharati MK (2010) Producing of AZ91/SiC composite by friction stir processing (FSP). Int J Adv Manuf Technol 51:247–260
10. Asadi P, Besharati Givi MK, Parvin N, Araei A, Taherishargh M, Tutunchilar S (2012) On the role of cooling and tool rotational direction on microstructure and mechanical properties of friction stir processed AZ91. Int J Adv Manuf Technol 63:987–997
11. Morisada Y, Fujii H, Nagaoka T, Fukusumi M (2006) MWCNTs/AZ31 surface composites fabricated by friction stir processing. Mat Sci Eng A 419:344–348
12. Chang CI, Wang YN, Pei HR, Lee CJ, Du CH, Huang JC (2007) Microstructure and mechanical properties of nano-ZrO2 and nano-SiO2 particulate reinforced AZ31-Mg based composites fabricated by friction stir processing. Key Eng Mat Comp Mat 351:114–119
13. Chang CI, Wang YN, Pei HR, Lee CJ, Huang (2006) On the hardening of friction stir processed Mg-AZ31 based composites with 5–20 % nano-ZrO2 and nano-SiO2 particles. Mat Trans 47: 2942–2949
14. Arora HS, Singh H, Dhindaw BK (2012) Composite fabrication using friction stir processing—a review. Int J Adv Manuf Technol 61:1043–1055
15. Elangovan K, Valliappan M, Balasubramanian V (2008) Influences of tool pin profile and axial force on the formation of friction stir processing zone in AA6061 aluminium alloy. Int J Adv Manuf Technol 38:285–295
16. Xing H, Cao X, Wanping H et al (2005) Interfacial reactions in 3D-SiC network reinforced Cu-matrix composites prepared by squeeze casting. Mater Lett 59:1563–1566
17. Ramesh CS, Noor Ahmed R, Mujeebu MA, Abdullah MZ (2009) Development and performance analysis of novel cast copper–SiC–Gr hybrid composites. Mater Des 30(6):1957–1965
18. Bajwa S, Rainforth WM, Lee WE (2005) Sliding wear behaviour of SiC–Al_2O_3 nanocomposites. Wear 259:553–561